Electronic Supplementary Information for

Toward Highly Sensitive Surface-Enhanced Raman Scattering: The Design of 3D Hybrid System with Monolayer Graphene Sandwiched between Silver Nanohole Arrays and Gold Nanoparticles

Yuan Zhao,[*ab] Dong Yang,[b] Xiyu Li,[b] Yu Liu,[b] Xiang Hu,[c] Dianfa Zhou,[c] and Yalin Lu[*bcde]

[a]School of Physics and Optoelectronic Engineering, Ludong University, Yantai 264025, China.

[b]School of Chemistry and Materials Science, University of Science and Technology of China, Hefei, 230026, China

[c]Hefei National Laboratory for Physical Sciences at the Microscale, University of Science and Technology of China, Hefei, 230026, China

[d]Synergetic Innovation Center of Quantum Information & Quantum Physics, University of Science and Technology of China, Hefei 230026, China

[e]Laser Optics Research Center, Physics Department, United States Air Force Academy, Colorado 80840, USA

Email: yzhaol@mail.ustc.edu.cn, yllu@ustc.edu.cn

Yuan Zhao and Dong Yang contributed equally to this paper.

Supporting figures

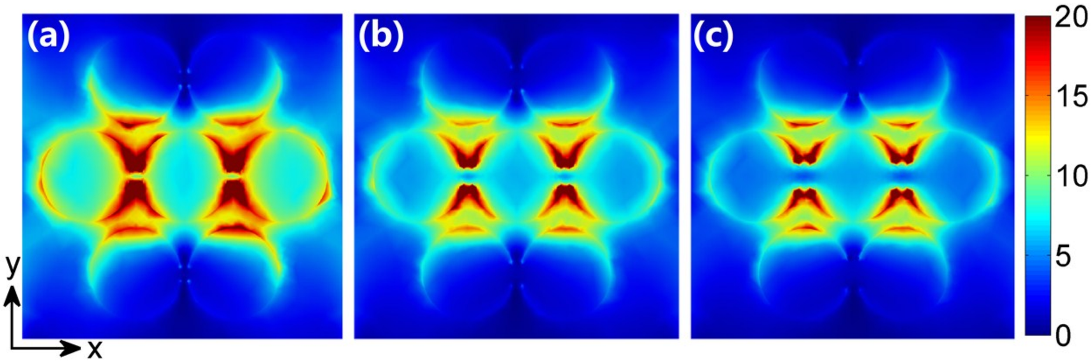

Fig. S1 Normalized electric field intensity distributions in the xy plane for communicating Ag NH arrays with Ag tip gaps to be (a) 17 nm, (b) 36 nm and (c) 51 nm, respectively.

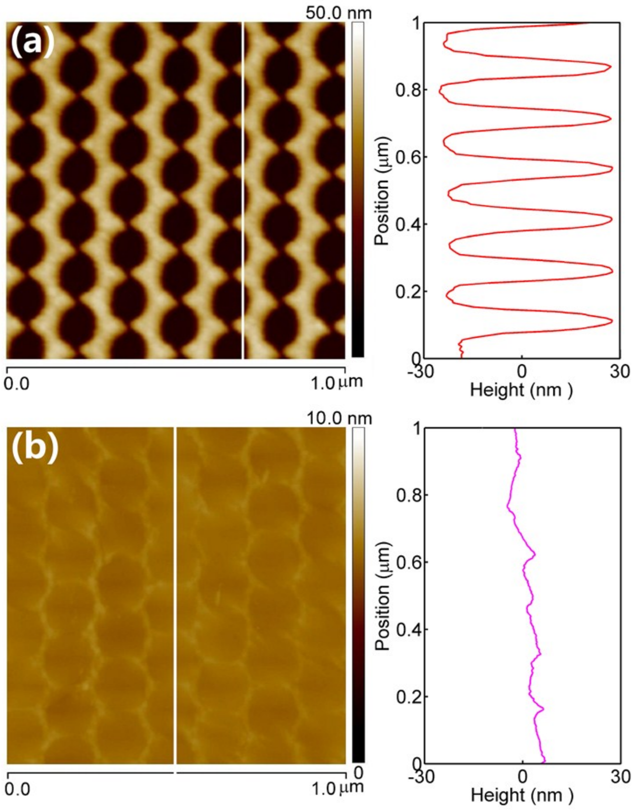

Fig. S2 AFM images of (a) Ag NH arrays and (b) 1LG-Ag NH array structures, respectively. The right images show the cross-sections along the white lines on the left.

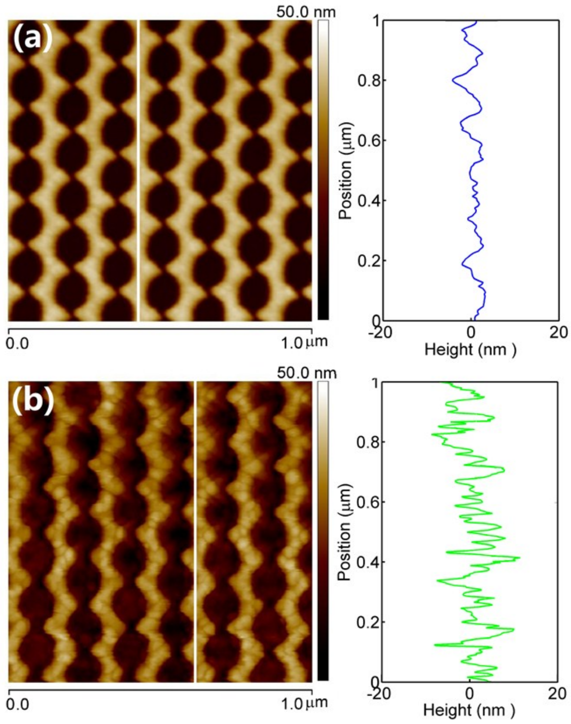

Fig. S3 AFM images of (a) Ag NH arrays and (b) Au NP-Ag NH array structures, respectively. The right images show the cross-sections along the white lines on the left.

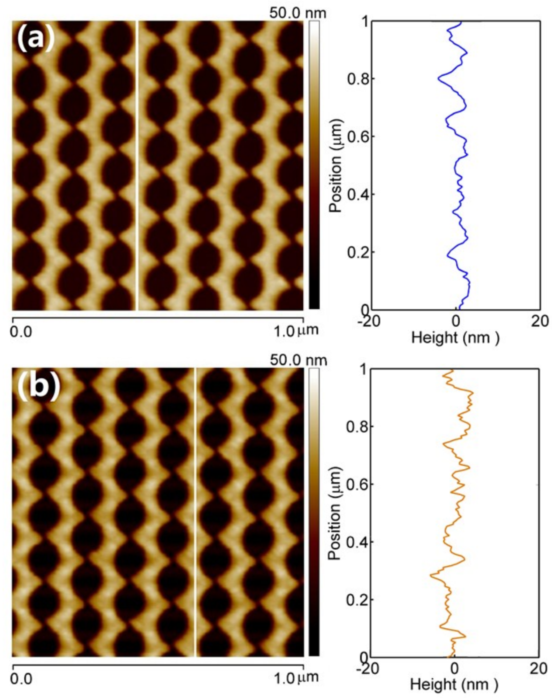

Fig. S4 AFM images of Ag NH arrays (a) before and (b) after annealing, respectively. The right images show the cross-sections along the white lines on the left.

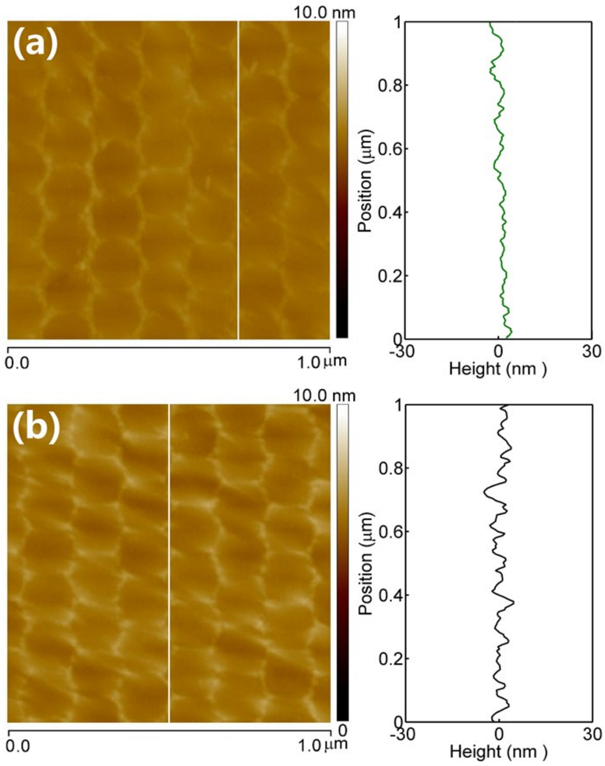

Fig. S5 AFM images of 1LG-Ag NH array structures (a) before and (b) after annealing, respectively. The right images show the cross-sections along the white lines on the left.

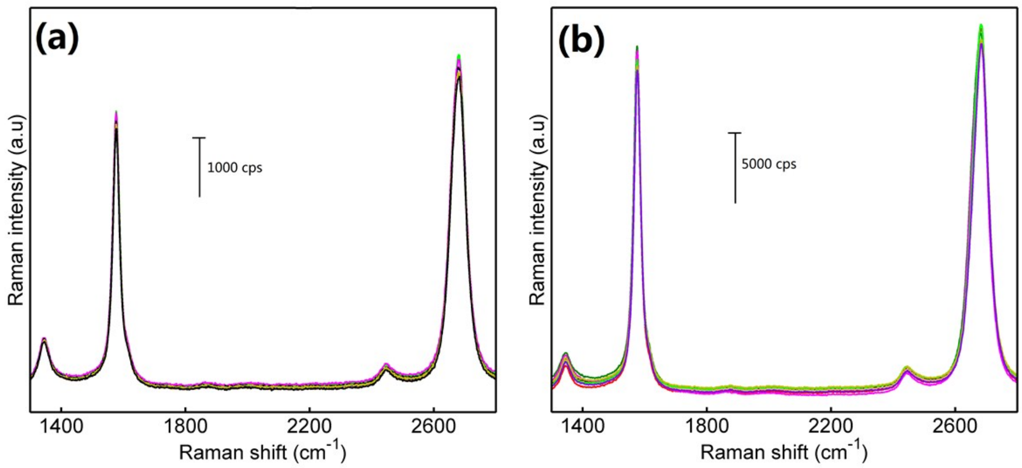

Fig. S6 SERS spectra of monolayer graphene (a) on Ag NH arrays and (b) sandwiched between Au NPs and Ag NH arrays collected from 8 random spots.

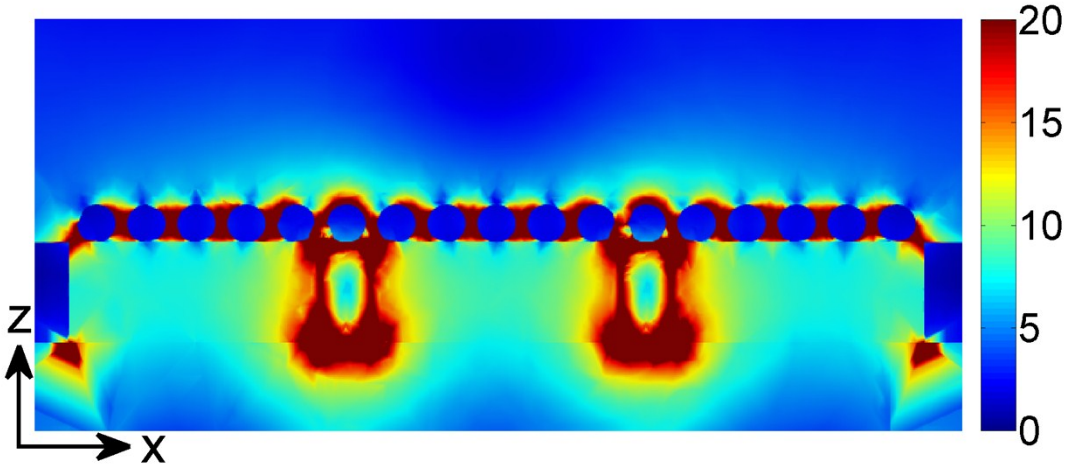

Fig. S7 Normalized electric field intensity distribution in the xz plane for Au NP-1LG-Ag NH array structure with graphene sandwiched between Au NPs and communicating Ag NH arrays.

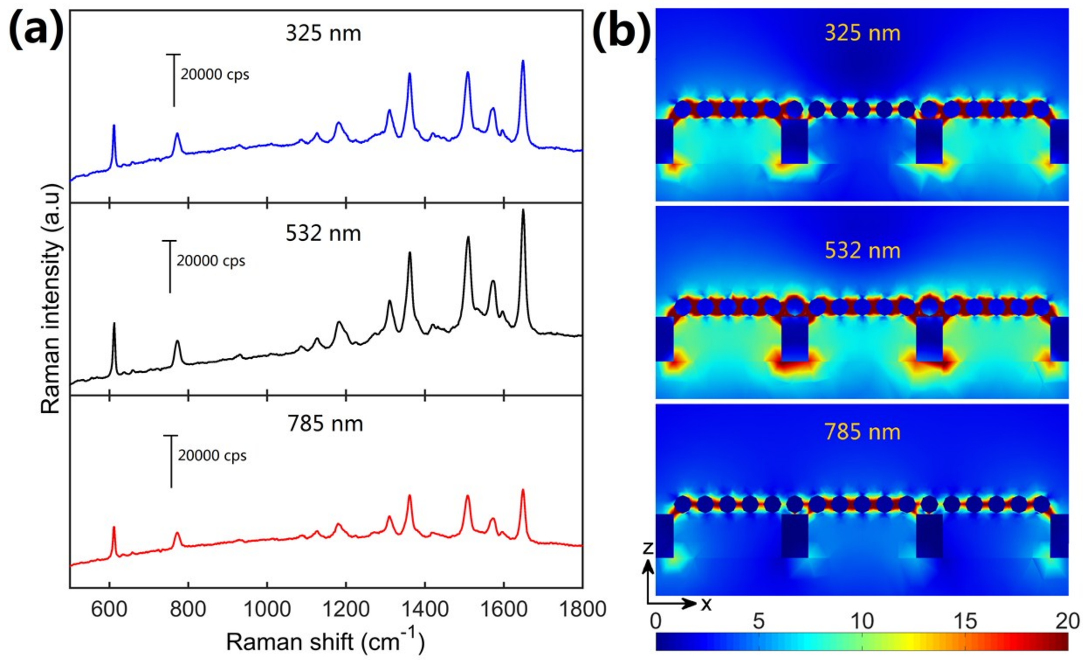

Fig. S8 (a) SERS spectra of 10^{-8} M R6G on Au NP-1LG-Ag NH array structure with excitation wavelength of 325 nm, 532 nm and 785 nm, respectively. (b) Normalized electric field intensity distributions of Au NP-1LG-Ag NH array structure in the xz plane with excitation wavelength of 325 nm, 532 nm and 785 nm, respectively.

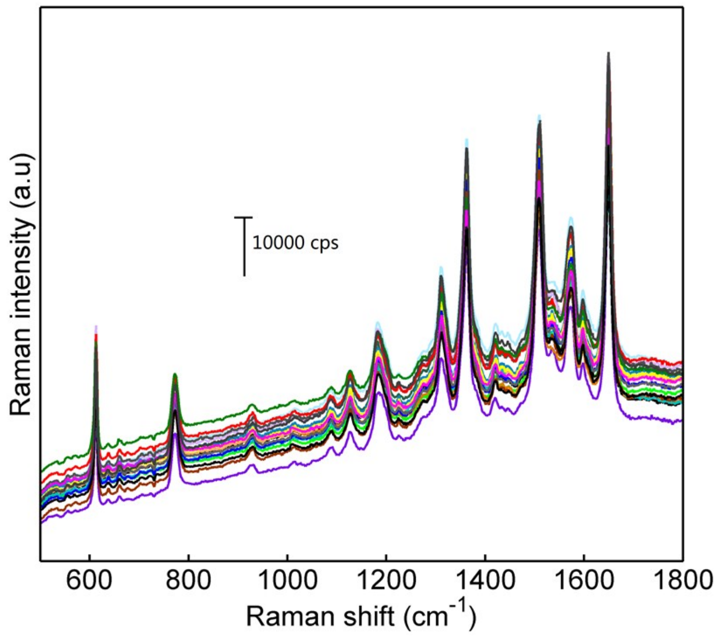

Fig. S9 SERS spectra of 10^{-8} M R6G on Au NP-1LG-Ag NH array structure collected from 20 random spots.

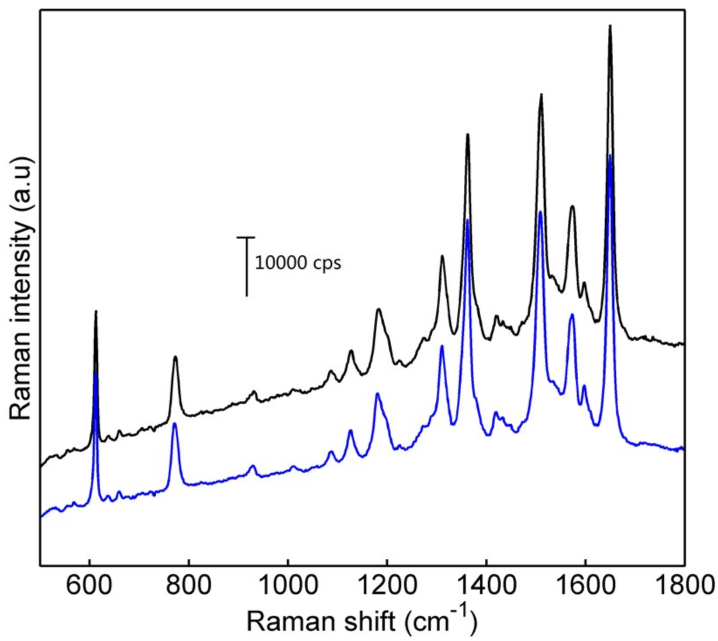

Fig. S10 SERS spectra of 10^{-8} M R6G on Au NP-1LG-Ag NH array structure measured after two days (black lines) and five months (blue lines) since the sample was prepared.

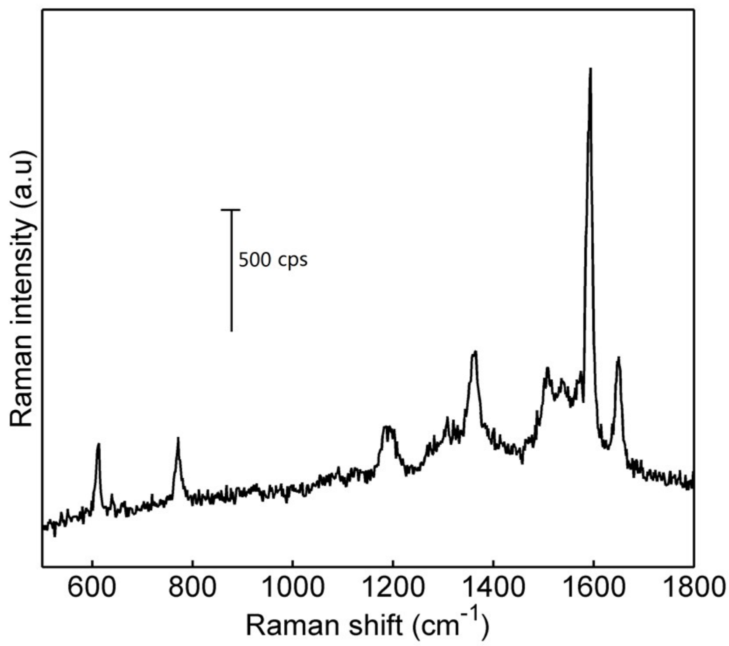

Fig. S11 SERS spectrum of 10^{-13} M R6G on Au NP-1LG-Ag NH array structure.

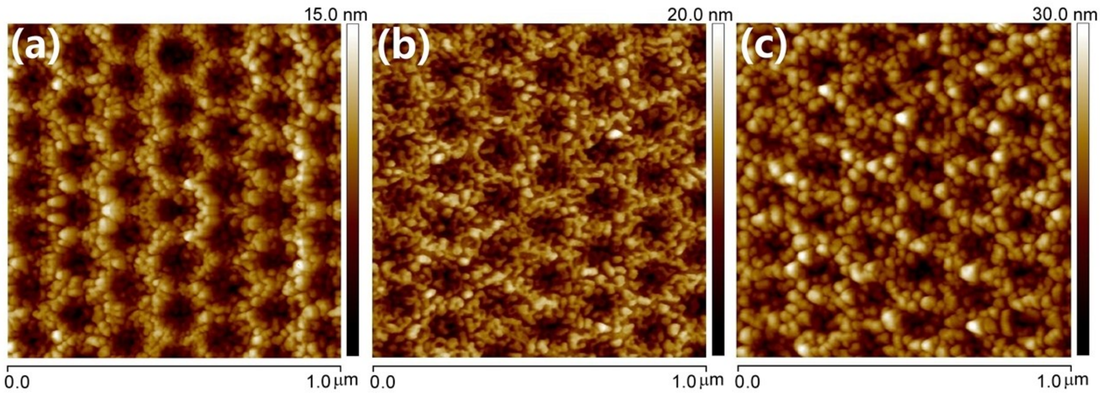

Fig. S12 AFM images of Au NP-1LG-Ag NH array structures obtained by depositing and annealing (a) 3, (b) 5, and (c) 8 nm-thick Au film on 1LG-Ag NH array structures, giving an diameter of ~ 12 nm and a particle density of 2674/µm^2 for annealing 3 nm-thick Au film; an diameter of ~ 20 nm and a particle density of 1521/µm^2 for annealing 5 nm-thick Au film; an diameter of ~ 32 nm and a particle density of 565/µm^2 for annealing 8 nm-thick Au film, respectively.

The effective diameter of Au NPs is estimated as the diameter of a circle surrounding the particle.

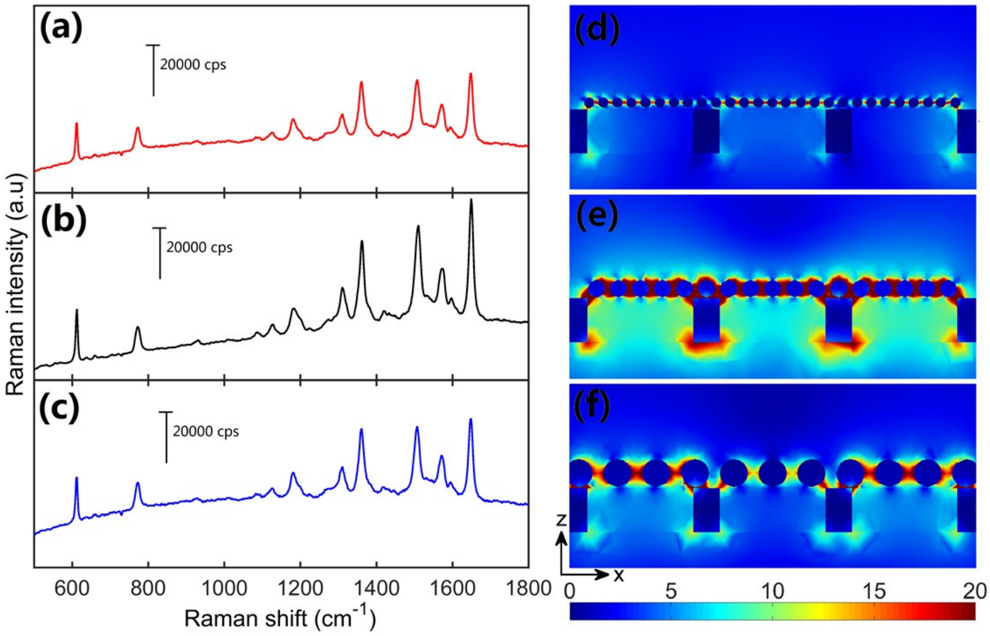

Fig. S13 SERS spectra of 10^{-8} M R6G on three different Au NP-1LG-Ag NH array structures obtained by depositing and annealing (a) 3, (b) 5, and (c) 8 nm-thick Au film on 1LG-Ag NH array structures. Normalized electric field intensity distributions of Au NP-1LG-Ag NH array structures in the xz plane at 532 nm with the diameter of Au NPs and distance between the adjacent Au NPs to be (d) 12 nm, 16 nm; (d) 20 nm, 25 nm and (d) 32 nm, 44 nm, respectively.